Journal of Energy and Power Engineering 14 (2020) 225-232
doi:10.17265/1934-8975/2020.07.002

Modeling and Simulation of Nine-Phase Permanent Magnet Synchronous Motor

Xiaohan Zhang, Wei Xie and Peiwen Dou
Department of Electrical Engineering, Shanghai Maritime University, Shanghai 201306, China

Abstract: To study the operation characteristics of the nine-phase PMSM (Permanent Magnet Synchronous Motor), this paper derived the Clarke transformation matrix of the nine-phase PMSM with the winding 3Y shifted by 20° via analyzing the harmonic subspace of the multi-phase PMSM, and further obtained its mathematical model under the rotating coordinate system. Then, a nine-phase PMSM based on the proposed model was built in SIMULINK and the operation mode of starting, braking and phase missing is simulated. The simulation results show that the nine-phase PMSM has good dynamic performance and steady-state performance, which also verifies the correctness and rationality of the motor model.

Key words: Nine-phase PMSM, coordinate transformation, mathematical model, dynamic simulation.

1. Introduction

In recent years, with the fast development of microprocessor technology and control theory, multi-phase speed regulation system has gradually attracted people's attention and shows great potential in electric locomotive, large ship drive, aerospace and other occasions [1, 2]. Compared with the traditional three-phase motor drive system, multi-phase motor drive system has the significant advantages which can be concluded as the following three aspects: (1) Stable output torque; (2) The bridge arm of a single inverter carries relatively small power which can achieve high-power output under low-voltage conditions; (3) High reliability, small torque ripple and high fault tolerance rate.

Multi-phase motors are now widely used in high-power drives, such as super high-speed elevators, turbo compressor, and MW-class marine power grid generators. The nine-phase permanent magnet motor not only has the advantages of multi-phase motor, but also has the characteristics of high torque density and wide speed range of permanent magnet motor, which shows high application value. This article mainly researches on the modeling and simulation of nine-phase PMSM (Permanent Magnet Synchronous Motor). The simulation results show that the structure of nine-phase PMSM can effectively reduce the torque ripple and motor loss as well as increase the motor capacity.

2. Mathematical Model of Nine-Phase PMSM

The modeling method based on multi-dimensional space vector decoupling theory is suitable for mathematical modeling of any symmetrical multi-phase motor. The basic principle is to decompose the *n*-dimensional space of the multi-phase motor in natural coordinate into several orthogonal two-dimensional subspaces through space vector decomposition. Then, the system will be transformed to the rotating coordinate system with the rotor position as the reference by rotating coordinate change. At this time, if the stator winding is assumed to be an ideal symmetrical sinusoidal winding, the inductance matrix can be transformed into a diagonal matrix and there will be no coupling between the various harmonic subspaces.

Corresponding author: Wei Xie, Ph.D., professor, research fields: power electronic, drive control system and optimization design.

2.1 Model in Natural Coordinate System

In order to establish the mathematical model of the multiphase motor in the rotating coordinate system, we first analyze the voltage and the torque equation in natural coordinate system. Take an n-phase PMSM as an example, assuming:

(1) The winding resistance of each phase is equal and the structure is the same.

(2) The effects of iron core hysteresis and eddy currents are ignored.

(3) The skin effect and the temperature effect of the conductor are ignored.

(4) The secondary factors such as damper windings and the eddy currents in magnets are not considered.

Then in the natural coordinate system, the stator voltage equation, torque equation and motion equation of the n-phase PMSM can be expressed by Eqs. (1) to (4).

$$\boldsymbol{u} = \boldsymbol{R}\boldsymbol{i} + p\boldsymbol{\psi}(i,\theta) \tag{1}$$

$$\boldsymbol{\psi}(i,\theta) = \boldsymbol{L}_s + \boldsymbol{\psi}_r(\theta) \tag{2}$$

$$T_e = P\left(\frac{1}{2} i^T \cdot \frac{dL_s}{d\theta} \cdot i + i^T \cdot \frac{d\boldsymbol{\psi}_r(\theta)}{d\theta}\right) + T_c(\theta) \tag{3}$$

$$\mathrm{J}\frac{d\omega}{dt} = P(T_e - T_L) \tag{4}$$

where,

u is the phase voltage vector of the stator;

i is the phase current vector of the stator;

θ is the position angle of the rotor;

R is the diagonal matrix composed of phase resistance;

$\psi(i,\theta)$ is the flux vector of the stator winding;

L_s is the inductance matrix of the stator winding;

$\psi_r(\theta)$ is the flux vector with no-load;

T_e , $T_c(\theta)$, T_L are the electromagnetic torque, cogging torque and load torque respectively;

J is the moment of inertia of the system;

ω is the electrical angular velocity of the rotor;

$p = d/dt$ is the differential operator;

P is the number of pole pairs of the motor.

2.2 Coordinate Transformation

2.2.1 Air Gap Magnetomotive Force of Multi-phase PMSM

From the perspective of magnetomotive force, the basic working principle of a rotating electric machine is to generate a constant electromagnetic torque through the interaction of the stator's and the rotor's magnetomotive force [3]. Thus, to simplify the analysis, the following assumptions are made：

(1) The relative permeability of the iron core is infinite; the magnetic saturation effect can be ignored so that the magnetic circuit is linear and applicable to the superposition principle.

(2) The cogging is ignored; the inner surface of the stator is smooth;

(3) The winding currents are concentrated on a point in the inner circle of the stator;

(4) The core hysteresis and eddy current effects are ignored;

(5) The skin effect and the temperature effects of conductive materials are ignored;

(6) The motor speed is constant [4].

Take a nine-phase PMSM with 3Y shifted 20° winding as an example to analyze the magnetic potential wave of its stator winding. Without considering the saturation of the iron core, the magnetomotive force wave is linear. According to the winding function method, the magnetomotive force waveform can be decomposed into harmonics for separate analysis by Fourier decomposition. The magnetic potential generated at the position of ϕ in the air gap when the current $i(t)$ is applied to the winding of the x-th phase can be expressed by the product of the winding function and the current:

$$F_x(\phi,t) = N(\phi) \cdot i(t) \tag{5}$$

where, $N(\phi)$ is the winding function.

It can be seen from Eq. (5) that the air gap magnetic potential is a space-time function determined by the distribution and the current waveform of the windings. The spatial distribution of the windings is represented by the winding function, which also determines the waveform of the motor's back electromotive force. The Fourier decomposition of winding function is the main method of harmonic analysis of air gap magnetic potential. The winding function and current function can be expressed in the form of Fourier series [5], as in:

$$\begin{cases} N(\phi) = \sum_{\nu=1}^{\infty}\left[N_\nu \cdot cos\big(\nu(\phi - 2\pi(x-1)/m)\big)\right] \\ i(t) \ = \sum_{\mu=1}^{\infty}\left[I_\mu \cdot cos\big(\mu(\omega t - 2\pi(x-1)/m)\big)\right] \end{cases} \tag{6}$$

where,

N_ν is the amplitude of the ν-th harmonic of the winding function.

I_μ is the amplitude of the μ-th harmonic of the current function.

The magnetomotive force function produced by the interaction of the ν-th harmonics of the winding and the μ-th harmonics current of the current in the x-th phase winding can be expressed as Eq. (7).

$$F_{x\nu\mu}(\phi, t) = N_\nu I_\mu cos\big(\nu(\phi - 2\pi(x-1)/m)\big)cos\big(\mu(\omega t - 2\pi(x-1)/m)\big) \tag{7}$$

Thus, the combined magnetic potential of the ν-th winding harmonics and the μ-th current harmonics of all phase windings of multi-phase motors can be expressed as Eq. (8):

$$\begin{aligned} F_{\nu\mu}(\phi, t) &= \sum_{x=1}^{m} N_\nu I_\mu cos\big(\nu(\phi - 2\pi(x-1)/m)\big) \cdot cos\big(\mu(\omega t - 2\pi(x-1)/m)\big) \\ &= \sum_{x=1}^{m} \frac{1}{2} N_\nu I_\mu \begin{pmatrix} cos(\nu\phi + \mu\omega t - 2\pi(\nu+\mu)\,(x-1)/m) \\ +cos(\nu\phi - \mu\omega t - 2\pi(\nu-\mu)\,(x-1)/m) \end{pmatrix} \end{aligned} \tag{8}$$

Use Eq. (9) to uniformly express the summing polynomial in Eq. (8) and then Eq. (8) can be written as Eq. (10).

$$S_m = \sum_{x=1}^{m} cos\left(n \cdot \frac{x \cdot 2\pi}{m} + \phi_0\right) \tag{9}$$

$$F_{\nu\mu}(\phi, t) = \frac{1}{2} N_\nu I_\mu \left(\sum_{x=1}^{m} \cos\left(n_1 \cdot \frac{x \cdot 2\pi}{m} + \phi_{01}\right) + \sum_{x=1}^{m} \cos\left(n_2 \cdot \frac{x \cdot 2\pi}{m} + \phi_{02}\right)\right) = \frac{1}{2} N_\nu I_\mu (S_{m1} + S_{m2}) \tag{10}$$

where, $n_1 = \nu + \mu$; $n_2 = \nu - \mu$.

It can be seen from Eq. (9) that when n satisfies the equation $n = k \cdot m\ (k = 0,\ \pm1,\ \pm2,\ \pm3 \ldots)$, $S_m = m\cos(\varphi_0)$; when n satisfies the equation $n \neq k \cdot m\ (k = 0,\ \pm1,\ \pm2,\ \pm3 \ldots)$, $S_m = 0$. Thus, Eq. (10) can be further simplified to solve the relationship between the combined magnetic potential $F_{\nu\mu}$, the winding harmonic order ν and the current harmonic order μ, as in Table 1 [6], where k, l can be any integer.

It can be seen from Table 1 that only when the winding harmonic order ν and the current harmonic order μ satisfy $\nu + \mu \neq k \cdot m$ and $\nu - \mu = l \cdot m$, the synthetic magnetomotive force $F_{\nu\mu}$ rotates in the same direction of the fundamental magnetomotive force.

2.2.2 Coordinate Transformation Matrix

The generalized Clarke transformation of equal amplitude for a symmetric 18-phase motor can be expressed as Eq. (11).

$$T_{18s/2s} = \left(\frac{1}{9}\right)\begin{bmatrix} 1 & cos20° & cos2\times20° & L & cos16\times20° & cos17\times20° \\ 0 & sin20° & sin2\times20° & L & sin16\times20° & sin17\times20° \\ 1 & cos40° & cos4\times20° & L & cos32\times20° & cos34\times20° \\ 0 & sin40° & sin4\times20° & L & sin32\times20° & sin34\times20° \\ M & M & M & & M & M \\ 1 & cos8\times20° & cos16\times20° & L & cos128\times20° & cos136\times20° \\ 0 & sin8\times20° & sin16\times20° & L & sin128\times20° & sin136\times20° \\ 1/\sqrt{2} & -1/\sqrt{2} & 1/\sqrt{2} & L & 1/\sqrt{2} & 1/\sqrt{2} \\ 1/\sqrt{2} & -1/\sqrt{2} & 1/\sqrt{2} & L & 1/\sqrt{2} & -1/\sqrt{2} \end{bmatrix} \tag{11}$$

In terms of the winding distribution characteristics of the stator windings of a nine-phase PMSM with three Y shifted by 20°, the nine-phase PMSM can be equivalently regarded as a half 18-phase motor. Considering that the actual nine-phase PMSM with three Y shifted by 20° only has the 1st, 2nd, 3rd, 7th, 8th, 9th, 13th, 14th, and 15th phase windings, as shown in Fig. 1, therefore we only need to extract the corresponding nine columns from Eq. (11) to form a transformation matrix with 18 rows and 9 columns. In addition, through the orthogonal subspace decomposition, the vector space of the symmetric 18-phase motor is decomposed into the fundamental subspace, the harmonic subspace and the subspace where the zero-sequence component is located. Then the distribution of the harmonics of the asymmetric nine-phase permanent magnet motor in the two-phase static model can be obtained, as shown in Table 2.

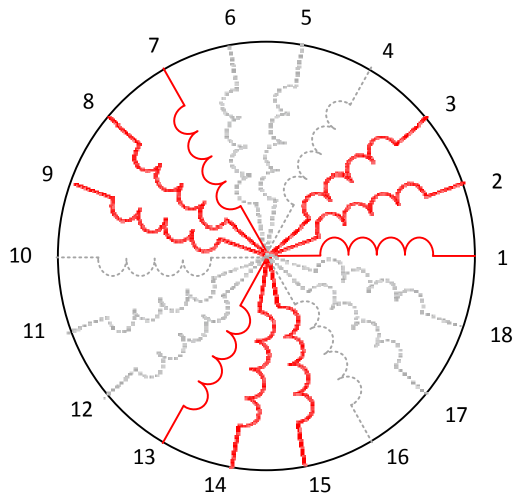

Fig. 1 Schematic diagram of windings of asymmetrical nine-phase PMSM.

Table 1 Relationship table between $F_{\nu\mu}$, ν and μ.

$F_{\nu\mu}$	Spatial characteristics of $F_{\nu\mu}$	Relationship between μ and ν
0	$F_{\nu\mu}$ equals to 0.	$n_1 = \nu + \mu \neq k \cdot m$ $n_2 = \nu - \mu \neq l \cdot m$
$\frac{mN_\nu I_\mu}{2} Ree^{j(\nu\phi - \mu\omega t)}$	$F_{\nu\mu}$ is in the same direction as the rotation direction of the fundamental magnetomotive force.	$n_1 = \nu + \mu \neq k \cdot m$ $n_2 = \nu - \mu = l \cdot m$
$\frac{mN_\nu I_\mu}{2} Ree^{j(\nu\phi + \mu\omega t)}$	$F_{\nu\mu}$ is opposite to the direction of rotation of the fundamental magnetomotive force.	$n_1 = \nu + \mu = k \cdot m$ $n_2 = \nu - \mu \neq l \cdot m$
$mN_\nu I_\mu cos(\mu\omega t) cos(\nu\phi)$	$F_{\nu\mu}$ is the pulsating standing wave.	$n_1 = \nu + \mu = k \cdot m$ $n_2 = \nu - \mu = l \cdot m$

Table 2 Harmonic group of each subspace.

μ	Subspace	Harmonic order
1	Fundamental subspace	1, 17, 19 … 18k±1
5	The subspace where the 5th harmonic locates	5, 13, 23 … 18k±5
7	The subspace where the 7th harmonic locates	7, 11, 25 … 18k±7
3, 9	Zero-sequence component subspace	3, 9, 15… 6k±3

Thus, Eq. (11) can be simplified as Eq. (12).

$$T_{2s/9s} = (2/9) \cdot \begin{bmatrix} 1 & cos20° & cos40° & -cos60° & -cos40° & -cos20° & -cos60° & -cos80° & cos80° \\ 0 & sin20° & sin40° & sin60° & sin40° & sin20° & -sin60° & -sin80° & -sin80° \\ 1 & cos60° & -cos60° & 1 & cos60° & -cos60° & 1 & cos60° & -cos60° \\ 0 & sin60° & sin60° & 0 & sin60° & sin60° & 0 & sin60° & sin60° \\ 1 & -cos80° & -cos20° & -cos60° & cos20° & cos80° & -cos60° & -cos40° & cos60° \\ 0 & sin80° & -sin20° & -sin60° & -sin20° & sin80° & sin60° & -sin40° & -sin60° \\ 1 & -cos40° & cos80° & -cos60° & -cos80° & cos40° & -cos60° & cos20° & -cos20° \\ 0 & sin40° & -sin80° & sin60° & -sin80° & sin40° & -sin60° & sin20° & sin20° \\ 1/\sqrt{2} & 1/\sqrt{2} & 1/\sqrt{2} & 1/\sqrt{2} & 1/\sqrt{2} & 1/\sqrt{2} & 1/\sqrt{2} & 1/\sqrt{2} & 1/\sqrt{2} \end{bmatrix} \quad (12)$$

According to the coordinate transformation principle of the three-phase motor, the Park transformation is only consistent with the vector rotation matrix in mathematical form. The Park transformation of the multi-phase motor transforms the physical quantities involved in the electromechanical energy conversion from the two-phase stationary coordinate system to two-phase rotating coordinate system. Therefore, the form of the rotation coordinate transformation matrix of the same subspace of the multi-phase motor is the same as that of the three-phase motor, and the rotation angle of the different order coordinates must be consistent with the rotation angle θ of the lowest harmonic vector in the subspace. Then, the rotation transformation matrix of a symmetrical nine-phase permanent magnet motor can be written as Eq. (13).

$$T_{2s/2r} = \begin{bmatrix} cos\theta & sin\theta & 0 & 0 & 0 & 0 & 0 & 0 & 0 \\ -sin\theta & cos\theta & 0 & 0 & 0 & 0 & 0 & 0 & 0 \\ 0 & 0 & cos3\theta & sin3\theta & 0 & 0 & 0 & 0 & 0 \\ 0 & 0 & -sin3\theta & cos3\theta & 0 & 0 & 0 & 0 & 0 \\ 0 & 0 & 0 & 0 & cos5\theta & sin5\theta & 0 & 0 & 0 \\ 0 & 0 & 0 & 0 & -sin5\theta & cos5\theta & 0 & 0 & 0 \\ 0 & 0 & 0 & 0 & 0 & 0 & cos7\theta & sin7\theta & 0 \\ 0 & 0 & 0 & 0 & 0 & 0 & -sin7\theta & cos7\theta & 0 \\ 0 & 0 & 0 & 0 & 0 & 0 & 0 & 0 & 1 \end{bmatrix} \tag{13}$$

Combined Eqs. (12) with (13), it can be obtained that the constant amplitude multi-dimensional rotating coordinate transformation matrix of the asymmetric nine-phase PMSM can be expressed as Eq. (14).

2.3 Model in Rotating Coordinate System

Based on the theories in Sections 2.1 and 2.2, we transform the vectors in each natural coordinate system to a multi-dimensional rotating coordinate system, and then the mathematical model of the motor in the rotating coordinate system can be calculated.

$$\begin{aligned} \boldsymbol{L}_{dq} &= T_{9s/2r}\boldsymbol{L}_s T_{9s/2r}^{-1} \\ &= \mathrm{diag}\left(L_d, L_q, L_{3d}, L_{3q}, L_{5d}, L_{5q}, L_{7d}, L_{7q}\right) \end{aligned} \tag{15}$$

$$\boldsymbol{i}_{dq} = T_{9s/2r}\boldsymbol{i} = i_d, i_q, i_{3d}, i_{3q}, i_{5d}, i_{5q}, i_{7d}, i_{7q} \tag{16}$$

$$\begin{aligned} \boldsymbol{u}_{dq} &= T_{9s/2r}\boldsymbol{u} \\ &= u_d, u_q, u_{3d}, u_{3q}, u_{5d}, u_{5q}, u_{7d}, u_{7q} \end{aligned} \tag{17}$$

After ignoring the coupling between the fundamental wave, the 5th harmonic and the 7th harmonic and removing the third zero-sequence component, the voltage equation under the multi-dimensional rotating coordinate system of the asymmetric nine-phase PMSM can be obtained as:

$$\begin{bmatrix} u_d \\ u_q \\ u_{5d} \\ u_{5q} \\ u_{7d} \\ u_{7q} \end{bmatrix} = R_s \begin{bmatrix} i_d \\ i_q \\ i_{5d} \\ i_{5q} \\ i_{7d} \\ i_{7q} \end{bmatrix} + \begin{bmatrix} L_d & 0 & 0 & 0 & 0 & 0 \\ 0 & L_q & 0 & 0 & 0 & 0 \\ 0 & 0 & L_{5d} & 0 & 0 & 0 \\ 0 & 0 & 0 & L_{5q} & 0 & 0 \\ 0 & 0 & 0 & 0 & L_{7d} & 0 \\ 0 & 0 & 0 & 0 & 0 & L_{7q} \end{bmatrix} \frac{d}{dt} \begin{bmatrix} i_d \\ i_q \\ i_{5d} \\ i_{5q} \\ i_{7d} \\ i_{7q} \end{bmatrix} + \omega \begin{bmatrix} -L_q i_q \\ L_d i_d \\ -5L_{5q} i_{5q} \\ L_{5d} i_{5d} \\ -7L_{7q} i_{7q} \\ L_{7d} i_{7d} \end{bmatrix} + \omega \begin{bmatrix} 0 \\ \psi_1 \\ 0 \\ \psi_5 \\ 0 \\ \psi_7 \end{bmatrix} \tag{18}$$

The torque equation can be obtained by the expansion of Eq. (9):

$$\begin{aligned} T_e = \frac{9}{2} \cdot \mathrm{P}\big[&\left(L_d - L_q\right) i_d i_q + \psi_1 i_q \\ &+ 5\left(L_{5d} - L_{5q}\right) i_{5d} i_{5q} \\ &+ 5\psi_5 i_{5q} \\ &+ 7\left(L_{7d} - L_{7q}\right) i_{7d} i_{7q} \\ &+ 7\psi_7 i_{7q}\big] \end{aligned} \tag{19}$$

3. Simulation and Analysis

In order to verify the validity and rationality of the model constructed in Section 2, this paper builds a simulation model of the nine-phase motor in the d-q coordinate system on the MATLAB/SIMULINK simulation platform, as shown in Fig. 2. The motor parameters are as follows [7, 8].

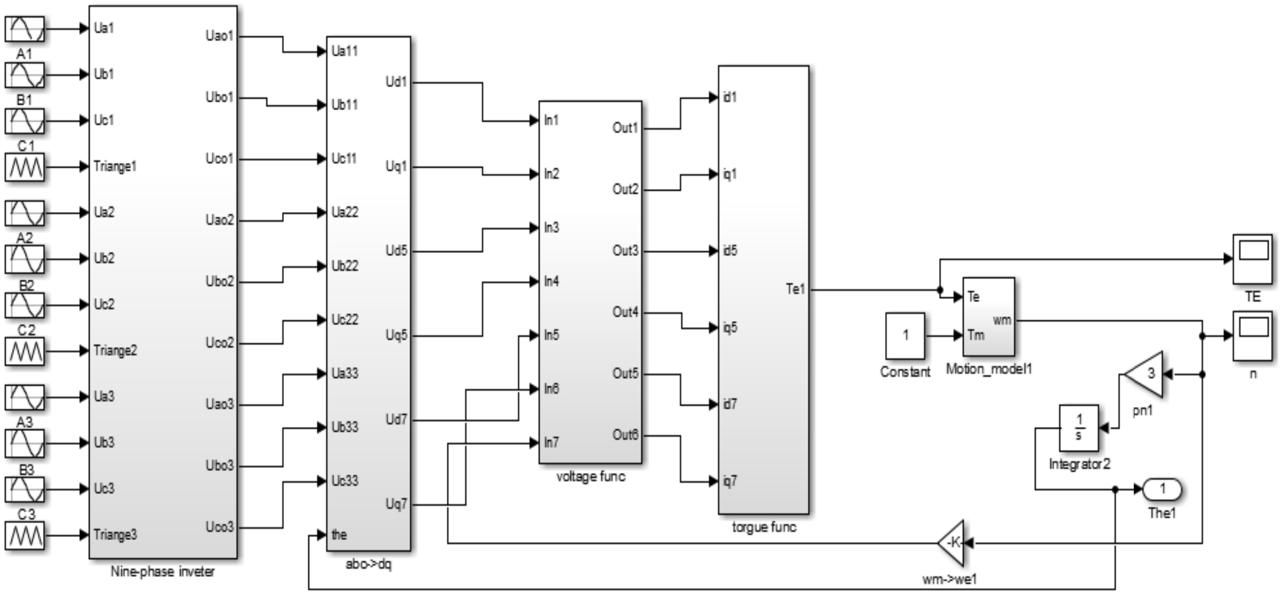

Fig. 2 Simulation model of nine-phase PMSM.

The stator resistance of each phase is 0.066 Ω; L_d, L_q, L_{5d}, L_{5q}, L_{7d} and L_{7q} are 0.0023 H, 0.0046 H, 0.0007 H, 0.0009 H, 0.0004 H and 0.0004 H, separately; ψ_1, ψ_5, ψ_7 are 0.1028 Wb, 0.07 Wb and 0.04 Wb, separately; the moment of inertia of the motor is $0.094\ \mathrm{kg \cdot m^2}$ and the number of pole pairs of the motor *P* is 3.

3.1 Start with No-Load and Operation with Load

From Fig. 3, the simulation results show that:

(1) The nine-phase PMSM has a faster response speed: the motor starts quickly and reaches the steady state after about 0.3 s.

(2) When starting with no load, the torque ripple and current ripple of the nine-phase PMSM are relatively large; when it reaches the steady state, the electromagnetic torque ripple and current ripple of the motor are small.

(3) The nine-phase PMSM has good steady-state performance: when the load is suddenly added after 0.8 s, the motor can quickly reach a new steady state again and the speed drop is small.

3.2 Dynamic Braking

After the nine-phase induction motor runs for 0.5 s with load, the stator phase winding A1 is energized with direct current, and the simulation result is shown in Fig. 4.

It can be seen from Fig. 4 that when the stator phase winding A1 is energized with the direct current, the nine-phase PMSM enters a state of energy consumption braking. In this state, the speed drops to zero quickly, the electromagnetic torque also becomes zero, and the current of the stator phase A1 suddenly increases and reaches a new value. After reaching a new steady state, it will gradually increase. The results show that the dynamic braking of the nine-phase PMSM is feasible.

3.3 Motor Running Out of Phase

When the motor is running stably, the power supply of phase A1 of the stator is disconnected at 0.9 s, and then the motor runs in a phase-loss state. From the simulation results shown in Fig. 5, it can be clearly seen that the speed only fluctuates and decreases slightly in the phase-loss mode, which is completely different from three-phase motors which cannot run when out of phase. Compared with 3-phase motor, the redundancy of the windings of the nine-phase PMSM greatly improves the reliability and stability of the system.

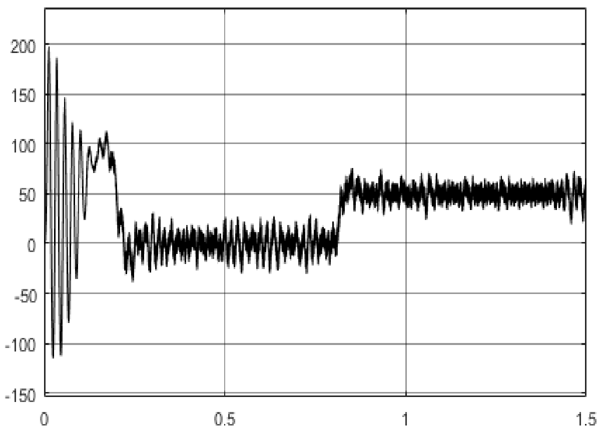

Fig. 3a Torque curve of no-load and with load.

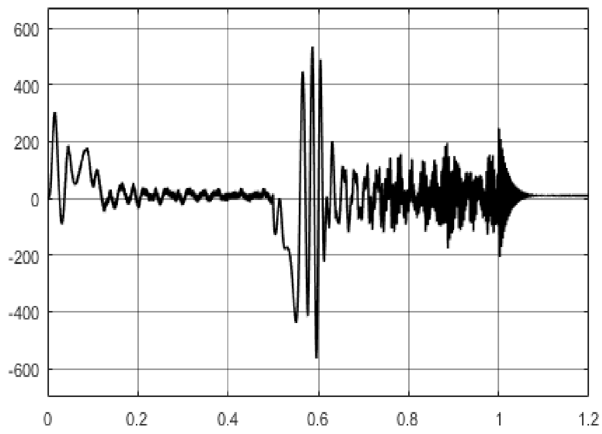

Fig. 4a Torque curve of dynamic braking.

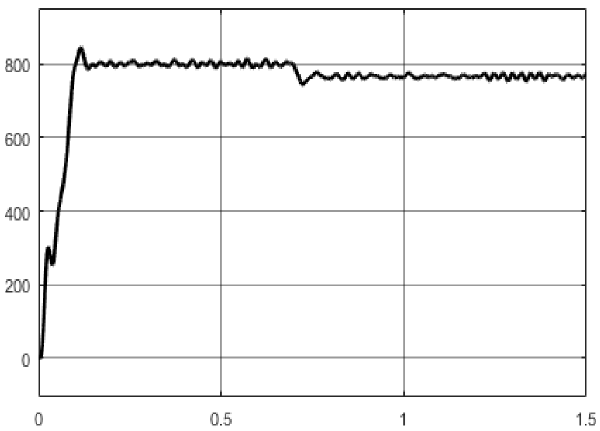

Fig. 3b Speed curve of no-load and with load.

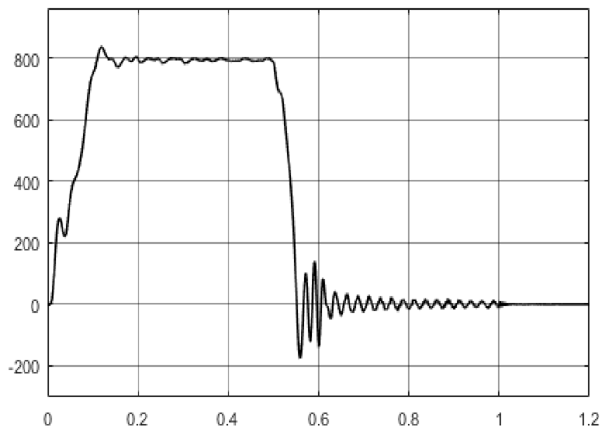

Fig. 4b Speed curve of dynamic braking.

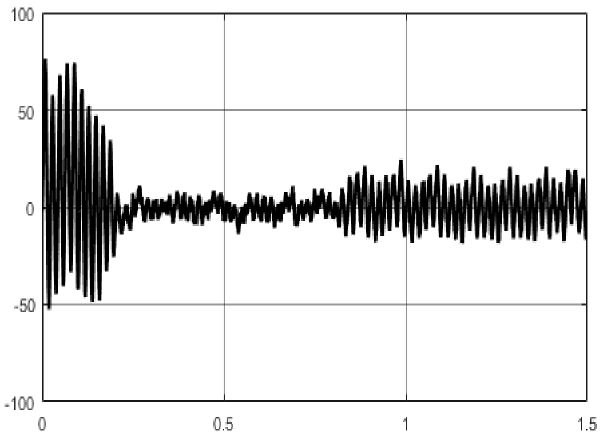

Fig. 3c A1 phase current curve of no-load and with load.

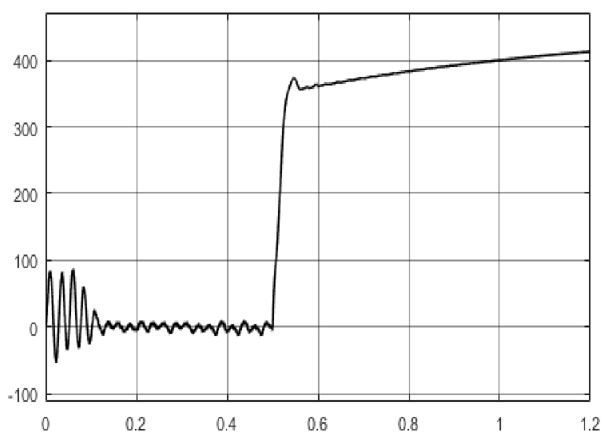

Fig. 4c A1 phase current curve of dynamic braking.

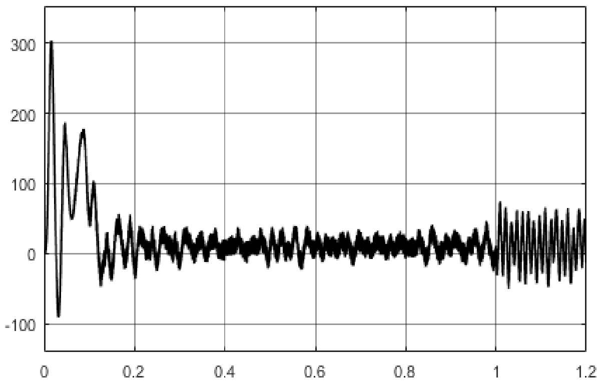

Fig. 5a Torque curve.

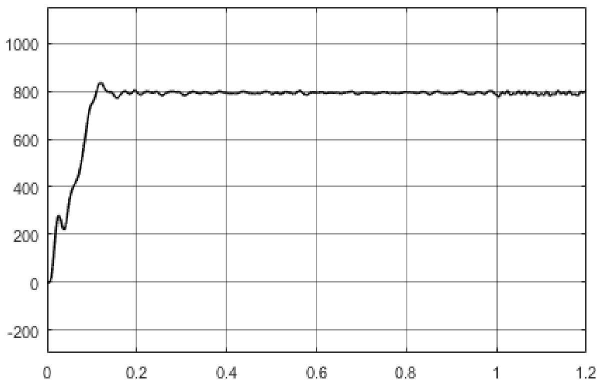

Fig. 5b Speed curve.

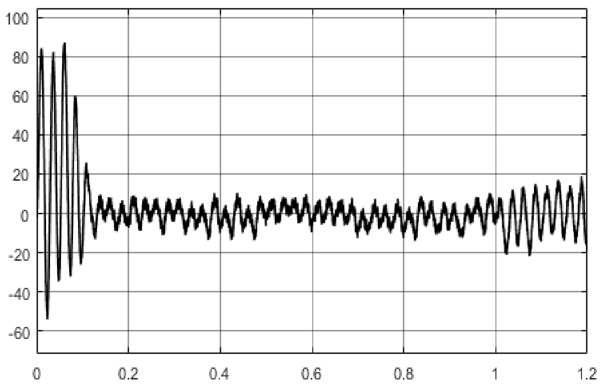

Fig. 5c A1 phase current curve.

4. Conclusion

This paper firstly completes the establishment of the mathematical model of the nine-phase permanent magnet motor in rotating coordinates by means of space vector decoupling theory. In order to verify the validity and rationality of the model, a simulation model of the speed control system of the asymmetrical nine-phase PMSM is built in the MATLAB/SIMULINK. Through the analysis of the simulation results in the starting, braking and phase-loss operation modes, it can be proved that the asymmetrical nine-phase permanent magnet motor has good dynamic performance and steady-state performance, as well as high reliability, small torque ripple and high fault tolerance.

References

[1] Levi, E. 2008. "Multiphase Electric Machines for Variable-Speed Applications." *Transactions on Industrial Electronics* 55: 1893-909.

[2] Wang, J. 2010. "Theoretical Analysis and Control Research of Multiphase Permanent Magnet Motor." Ph.D. thesis, Huazhong University of Science and Technology.

[3] Lyra, R. O. C., and Lipo, T. A. 2002. "Torque Density Improvement in a Six-Phaseinduction Motor with Third Harmonic Current Injection." *IEEE Transactions on Industry Application* 38: 1351-60.

[4] Toliyat, H. A., Lipo, T. A., and White, J. 1991. "Analysis of a Concentrated Winding Induction Machine for Adjustable Speed Drive Applications—Part II Machine Design and Performance." *IEEE Transactions on Energy Conversion.*

[5] Tang, H. 2013. "Research on Vector Control System of Nine Phase Induction Motor." M.Sc. thesis, Zhejiang University.

[6] Mei, B. S., and Xu, W. 2019. "Vector Control Strategy of Harmonic Injection Nine-Phase Permanent Magnet Synchronous Motor." *Electrical Measurement & Instrumentation* 18: 110-4.

[7] Xue, S., and Wen, X. H. 2006. "A Novel Multi-phase SVPWM." *Journal of Electrotechnical Technology* 21: 68-72.

[8] Bian, J. Y. 2015. "Research on Driving Technology of Nine-phase Permanent Magnet Motor for Ship Electric Propulsion." M.Sc. thesis, Huaqiao University.